




Cite this: *RSC Adv.*, 2025, 15, 25985

# A novel nanocatalyst praseodymium oxide ( $\text{Pr}_6\text{O}_{11}$ ) for the efficient and sustainable synthesis of chromene derivatives *via* ultrasound irradiation in an aqueous hydrotropic medium†

Sarika Patil,<sup>ab</sup> Nilesh Pandit,<sup>a</sup> Avdhut Kadam,<sup>a</sup> Suraj Attar,<sup>c</sup> Chaitali Bagade,<sup>d</sup> Dattaprasad Pore <sup>d</sup> and Santosh Kamble <sup>\*a</sup>

The development of sustainable and efficient catalytic methods for organic synthesis is a key focus in green chemistry. In this study, we report for the first time the novel application of praseodymium oxide ( $\text{Pr}_6\text{O}_{11}$ ) as a nanocatalyst for the eco-friendly synthesis of 2-amino-3-cyano-7-hydroxy-4*H*-chromenes. The hydrothermal synthesis of praseodymium oxide ( $\text{Pr}_6\text{O}_{11}$ ) nanoparticles was performed, and their structural studies were conducted using FTIR, XRD, TGA-DTA, SEM, EDX, BET, and TEM analysis. The  $\text{Pr}_6\text{O}_{11}$  NPs were used as a nanocatalyst in the synthesis of 2-amino-3-cyano-7-hydroxy-4*H*-chromenes. The reactions were conducted under ultrasound irradiation in an aqueous hydrotropic medium, eliminating the need for hazardous organic solvents. The unique catalytic properties of  $\text{Pr}_6\text{O}_{11}$  facilitated high yields of chromene derivatives, with excellent selectivity within short reaction times. The synergistic effect of ultrasound irradiation and hydrotrophy enhanced the reaction kinetics, leading to improved efficiency and sustainability. The catalyst exhibited remarkable reusability and stability, maintaining its activity over multiple cycles without any significant loss in efficiency. This novel approach highlights the potential of  $\text{Pr}_6\text{O}_{11}$  as a green and reusable nanocatalyst, offering a sustainable alternative for the synthesis of valuable heterocyclic compounds in aqueous hydrotropic media. The significant features of this method are the shorter reaction time, high product yield and use of a non-toxic, reusable, inexpensive, and biodegradable catalyst.

Received 2nd May 2025  
Accepted 22nd June 2025

DOI: 10.1039/d5ra03100a

rsc.li/rsc-advances

## 1. Introduction

The single-step synthesis of complex molecules is preferred with multicomponent reactions (MCRs), which represent a highly efficient, eco-friendly, and cost-effective synthetic approach.<sup>1–5</sup> MCRs also offer advantages such as atom economy, and selectivity, making them ideal for creating diverse compound libraries.<sup>6</sup> MCRs are already widely used in medicinal chemistry for drug discovery, as they allow the rapid assembly of molecular scaffolds with minimal time and effort. These reactions are valued for their simplicity, high yields, and environmental sustainability.<sup>7–9</sup>

Green chemistry is gaining popularity as a new approach followed in chemical processes and production to eliminate the

use and generation of hazardous substances completely or partially. It focuses on minimizing environmental impacts through safer, more sustainable practices,<sup>10</sup> such as using renewable resources, reducing waste, improving energy efficiency, and designing safer chemicals and processes. Green chemistry encourages innovation in synthetic methods, catalysts, and reaction conditions to promote sustainability and protect the environment.<sup>11–13</sup>

2-Amino-4*H*-chromene derivatives exhibit a wide range of pharmacological properties,<sup>14</sup> including antibacterial, antioxidant, solvatochromic,<sup>15</sup> and antitumor activities.<sup>16</sup> They also serve as essential scaffolds in biologically active compounds.<sup>17</sup> Additionally, these derivatives have demonstrated antimicrobial,<sup>18</sup> anticoagulant,<sup>19</sup> and anti-HIV<sup>20</sup> properties and have been employed as laser dyes,<sup>21</sup> as well as homogeneous and heterogeneous catalysts,<sup>22</sup> including solid-supported systems.<sup>23</sup> Despite their significance, there is still a need to improve the efficiency and sustainability of their synthesis. Typically, 2-amino-4*H*-chromene derivatives are synthesized *via* a one-pot condensation of aromatic aldehydes, malononitrile, and enolizable C–H-activated acidic compounds—a strategy that has gained attention due to its high atom economy and bond-forming efficiency.<sup>24</sup> These multicomponent reactions (MCRs)

<sup>a</sup>Department of Chemistry, Yashwantrao Chavan Institute of Science, Lead College, Karmaveer Bhaurao Patil University, Satara 415001, Maharashtra, India. E-mail: santosh.san143@gmail.com

<sup>b</sup>Department of Chemistry, S. G. M. College Karad, Satara 415001, Maharashtra, India

<sup>c</sup>Department of Chemistry, Shahajiraje Mahavidyalaya, Khatav, Satara, 415505, Maharashtra, India

<sup>d</sup>Department of Chemistry, Shivaji University, Kolhapur, 416004, Maharashtra, India

† Electronic supplementary information (ESI) available. See DOI: <https://doi.org/10.1039/d5ra03100a>



have been catalyzed by various homogeneous and heterogeneous systems, such as heteropolyacids,<sup>25</sup>  $K_2CO_3$ ,<sup>26</sup> potassium phthalimide,<sup>27</sup> cetyltrimethylammonium chloride,<sup>28</sup> nanosized  $MgO$ ,<sup>29</sup>  $\gamma$ -alumina,<sup>30</sup>  $Mg/Al$  hydrotalcite,<sup>31</sup>  $Fe(HSO_4)_3$ ,<sup>32</sup> DABCO entrapped in agar,<sup>33</sup>  $K_3PO_4$ ,<sup>34</sup> DBU,<sup>35</sup> and sulfonic acid-functionalized MIL-101(Cr),<sup>36</sup> all of which provide varying yields. However, many of these methods suffer from drawbacks, including tedious workups, costly catalysts and solvents, high temperatures, extended reaction times, and low product yields. Therefore, developing a simple, eco-friendly, and cost-effective protocol using a reusable catalyst for the one-pot synthesis of 2-amino-4*H*-chromene derivatives remains a compelling objective.

The use of aqueous media as solvents in organic reactions offers environmental benefits (non-toxic, biodegradable) and economic advantages<sup>37</sup> (low cost, easy disposal). Aqueous media provide unique reaction conditions, especially for polar compounds, but may have limitations, like poor solubility for nonpolar compounds and temperature constraints. Hydrotropes are water-soluble surface-active compounds that increase the solubility of organic molecules in water, often by up to 200 times, at higher concentrations. They consist of both hydrophilic and hydrophobic moieties but are typically too small to form micelles. The solubilizing effect of hydrotropes was first observed by Otto Neuberg in 1916.<sup>38</sup> Organic compounds are often insoluble in aqueous media, hindering reactions from completing. Hydrotropes like sodium *p*-toluene sulfonate (NaPTS) can enhance their solubility by solubilizing hydrophobic moieties in water. NaPTS is stable to air and moisture, non-toxic, and can be recycled several times. It has been selected in many studies, including herein, for its effectiveness and sustainability. Among hydrotropes, NaPTS is a preferred choice for facilitating aqueous reactions.<sup>39</sup> Herein, we report an

efficient synthesis of 2-amino-4*H*-chromene using  $Pr_6O_{11}$  NPs in an aqueous hydrotropic solution under ultrasonic irradiation.

$Pr_6O_{11}$  is the stable phase of praseodymium oxide in air at ambient temperature. It is a mixed-valent compound containing  $Pr^{3+}$  and  $Pr^{4+}$ . This oxide is more stable than other praseodymium oxides, like  $Pr_2O_3$  and  $PrO_2$ , under ambient conditions.<sup>40</sup>  $Pr_6O_{11}$  nanoparticles (NPs) have been used as catalysts in CO oxidation due to their redox properties and phase stability,<sup>41</sup> as well as electrical conductivity.<sup>42</sup> They are also effective in dye degradation through photocatalytic mechanisms.<sup>43</sup> Additionally,  $Pr_6O_{11}$  NPs synthesized by a precipitation method were used in the synthesis of 2-amino-4*H*-chromene derivatives, in a hydrotropic aqueous medium, showing their versatility in organic reactions.

Herein, we report for the first time a cost-effective, environmentally benign, and efficient procedure for the synthesis of  $Pr_6O_{11}$  NPs as a catalyst for chromene synthesis in a hydrotropic medium, leveraging their unique oxygen vacancies and Lewis acid properties. This reaction was catalyzed by  $Pr_6O_{11}$  NPs in a hydrotropic aqueous medium as it offers a green alternative for this transformation. Ultrasound irradiation in organic synthesis is a clean, energy-efficient alternative to conventional methods. It can enhance reaction rates, improve yields, and reduce the need for solvents, making it an environmentally friendly technique.<sup>44</sup> Ultrasound also promotes efficient mixing and generates localized high-energy conditions, making it a versatile tool for various synthetic transformations in organic chemistry.<sup>45</sup>

## 2. Materials and instruments

Analytical grade praseodymium metal, hydrochloric acid (HCl), potassium hydroxide (KOH), benzaldehyde, malononitrile, resorcinol, 20% NaPTS, ethyl acetate, and hexane were purchased from Sigma-Aldrich. Double-distilled water (DDW)

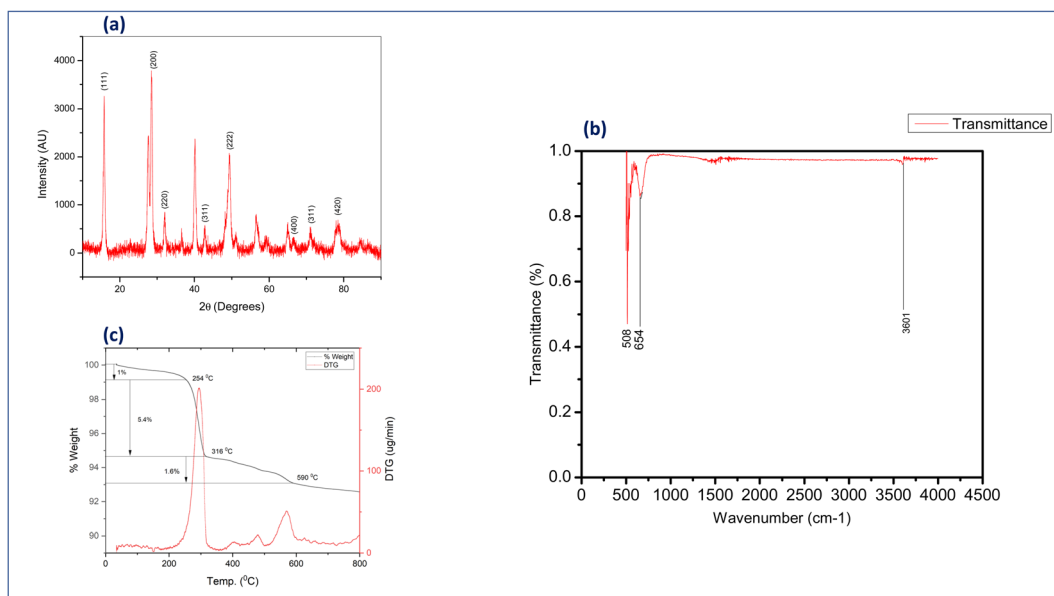


Fig. 1 (a) XRD pattern, (b) FTIR spectrum, and (c) TGA-DTA analysis of the prepared  $Pr_6O_{11}$  NPs.



was used as the solvent throughout. A stainless steel autoclave with a polytetrafluoroethylene (PTFE) container was used for the hydrothermal synthesis.

The XRD study was carried out using an X-ray diffractometer (Ultima IV Rigaku D/max2550Vb + 18 kw with  $\text{CuK}\alpha$ ,  $\lambda = 1.54056 \text{ \AA}$ ) in the range of diffraction angles ( $2\theta$ ) between  $10^\circ$  and  $90^\circ$ . The morphological analysis was performed by SEM (s-4300, Hitachi, Japan). The FTIR study was carried out using an FTIR spectrophotometer (Nicolet iS10, Thermo Scientific, USA) in the wavenumber range of  $400\text{--}4000 \text{ cm}^{-1}$ . Mass measurements were carried using an accurate analytical microbalance (Tapson 100 TS) with at least a count of  $10^{-5} \text{ mg}$ . The SAED patterns confirmed the plane orientations (JEOL JEM 1400 plus, Japan). Transmission electron microscopy (TEM) was carried out using a JEOL JEM-2100 plus system (Japan) at an accelerating voltage

of 200 kV equipped with a high-resolution CCD camera. For the Brunauer–Emmett–Teller (BET) surface area analysis and to determine the pore sizes of the material,  $\text{N}_2$  sorption isotherms were measured using a Metrohm BELSORP miniX instrument at 77 K with  $\text{N}_2$  as the adsorptive gas. Prior to the  $\text{N}_2$  sorption measurements, the samples were degassed at  $220^\circ \text{C}$  for 6 h to remove the moisture in the samples.

The surface morphologies and elemental compositions were analyzed by field emission scanning electron microscopy (FESEM) and elemental dispersive X-ray spectroscopy (EDX) using an FESEM + EDS analyzer (JEOL, JSM-7600F). NMR studies were carried out using a nuclear magnetic resonance spectrometer at 400 MHz (Bruker Biospin Switzerland, Ascend) and 750 MHz. Melting points were determined using digital melting/boiling point apparatus (EQ 730A EQUIPTRONICS).

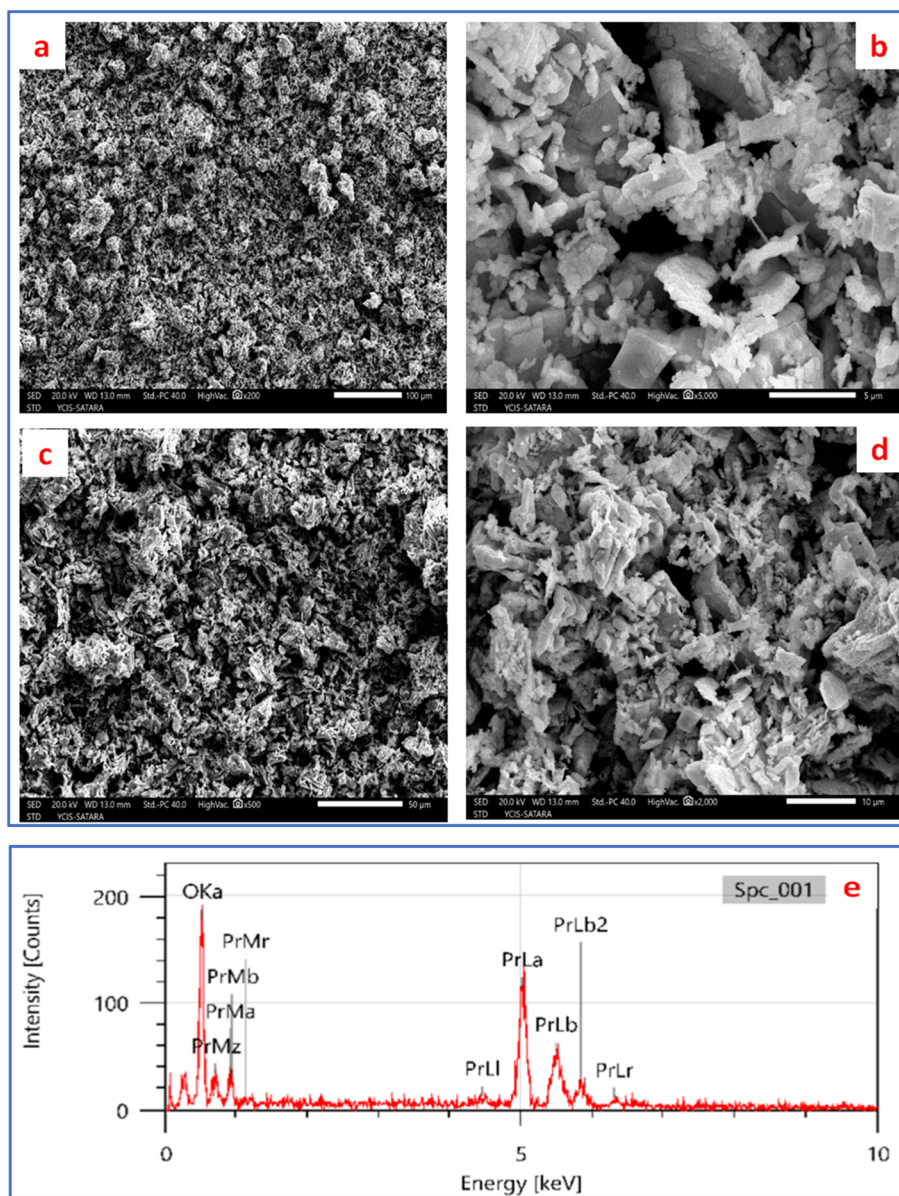


Fig. 2 (a–d) FESEM images at different magnifications; (e) EDX pattern of the prepared  $\text{Pr}_6\text{O}_{11}$  NPs.

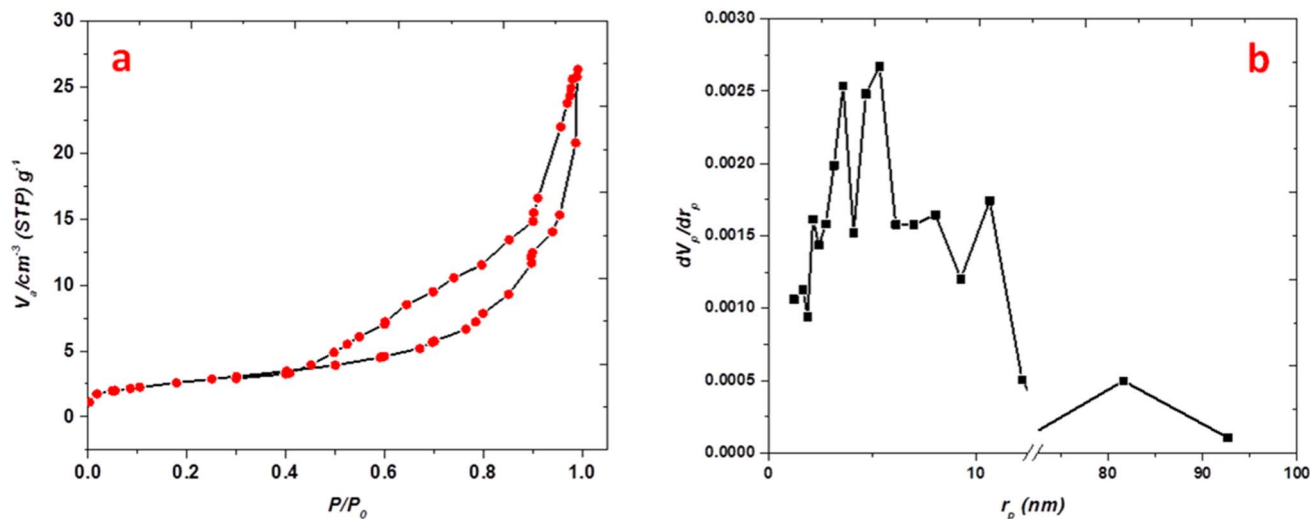


Fig. 3 BET analyses (a) adsorption–desorption (b) pore diameter of the prepared  $\text{Pr}_6\text{O}_{11}$ .

### 3. Experimental section

The experimental procedure comprised two steps: preparation of the praseodymium oxide nanoparticles ( $\text{Pr}_6\text{O}_{11}$  NPs) and synthesis of the chromene derivatives using the prepared NPs by ultrasound-assisted catalytic separation.

#### 3.1. Preparation of the $\text{Pr}_6\text{O}_{11}$ NPs by hydrothermal oxidation

Praseodymium metal powder (2 g) was dissolved in concentrated hydrochloric acid (5 mL) to form praseodymium chloride solution (0.1 M). An aqueous solution of 5 M KOH was added drop-wise into the 0.1 M praseodymium chloride solution under stirring at 800 r.p.m. until praseodymium hydroxide precipitated completely. The precipitate was aged for 15 min in air and then washed repeatedly with distilled water until the pH became 8 to remove  $\text{Cl}^-$  anions in the precipitate. Next, 40 mL of 5 M KOH was added to the wet precipitate under sonication in the ultrasonic bath. The treated precipitate was then subjected to hydrothermal treatment at 180 °C for 45 h in an autoclave. The solid was recovered and rinsed with deionized water until the pH value approached approximately 7. The as-obtained precipitate was dried at 60 °C for 1 day and then calcined at designated temperatures for 2 h in the air to convert the precipitate into oxide nanoparticles (NPs).

#### 3.2. Synthesis of 2-amino-3-cyano-7-hydroxy-4H-chromene

After successful synthesis of the  $\text{Pr}_6\text{O}_{11}$ , it was utilized for the catalytic separation of the chromene derivatives. In order to develop a green protocol and check the viability of the reaction in aqueous and partially alcoholic media, a long screening test involving various parameters, like the choice of catalyst, NaPTS, application of ultrasound frequencies, and the solvents being fully or partially aqueous, was carried out as part of the method development. The developed method was denoted as ‘model reaction 2’. Aqueous solutions of 0.101 mL of 1 mM

benzaldehyde, 0.063 mL of 1 mM malononitrile, 0.11 g of 1 mM resorcinol, and 20% NaPTS were added in a container. To these reactants, 0.01 g of 10 mol%  $\text{Pr}_6\text{O}_{11}$  NPs was added as a catalyst. These reactants were then subjected to ultrasonic irradiation (ultrasound frequency: 25 kHz; output power: 6.5–650 W) at room temperature for 5 min, and the progress of the reaction was monitored by TLC (ethyl acetate:hexane = 8:2). The product was filtered with Whatman filter paper no. 41 to separate the catalyst ( $\text{Pr}_6\text{O}_{11}$ ) NPs. The catalyst NPs were preserved for the recyclability test. The product devoid of catalyst obtained after filtration was re-crystallized by ethanol and characterized by  $^1\text{H}$  NMR and  $^{13}\text{C}$  NMR spectroscopy.

#### 3.3. Recyclability of the catalyst

To check whether the catalyst  $\text{Pr}_6\text{O}_{11}$  could be recycled or not, a recyclability study was carried out. Here, after each reaction, the catalyst was isolated by simple filtration, reactivated by cleaning with ethanol, and then dried in a hot air oven. The product was separated by filtering the solid after adding 15 mL of ice-cold water to the reaction mixture. The aqueous layer was recovered, and the organic reactant/product was extracted using ethyl acetate.

## 4. Results and discussion

#### 4.1. Structural study of the prepared catalyst

The structure and composition of the prepared catalyst were studied using various material characterization techniques, as described below.

**4.1.1. XRD analysis.** The prepared catalyst was subjected to XRD analysis. Various diffraction peaks were observed (Fig. 1a). The peaks were closely matched to those present in JCPDS data card 42-1121. Peaks were observed at  $2\theta$  values of 18.23°, 29.18°, 32.54°, 41.35°, 48.65°, 58.66°, 65.38°, 79.88°, oriented along the (111), (200), (220), (311), (222), (400), (311), and (420) planes, respectively. These peaks confirmed the formation of  $\text{Pr}_6\text{O}_{11}$  cubic structures with the space group  $Fd\bar{3}m$ .<sup>46</sup> The average





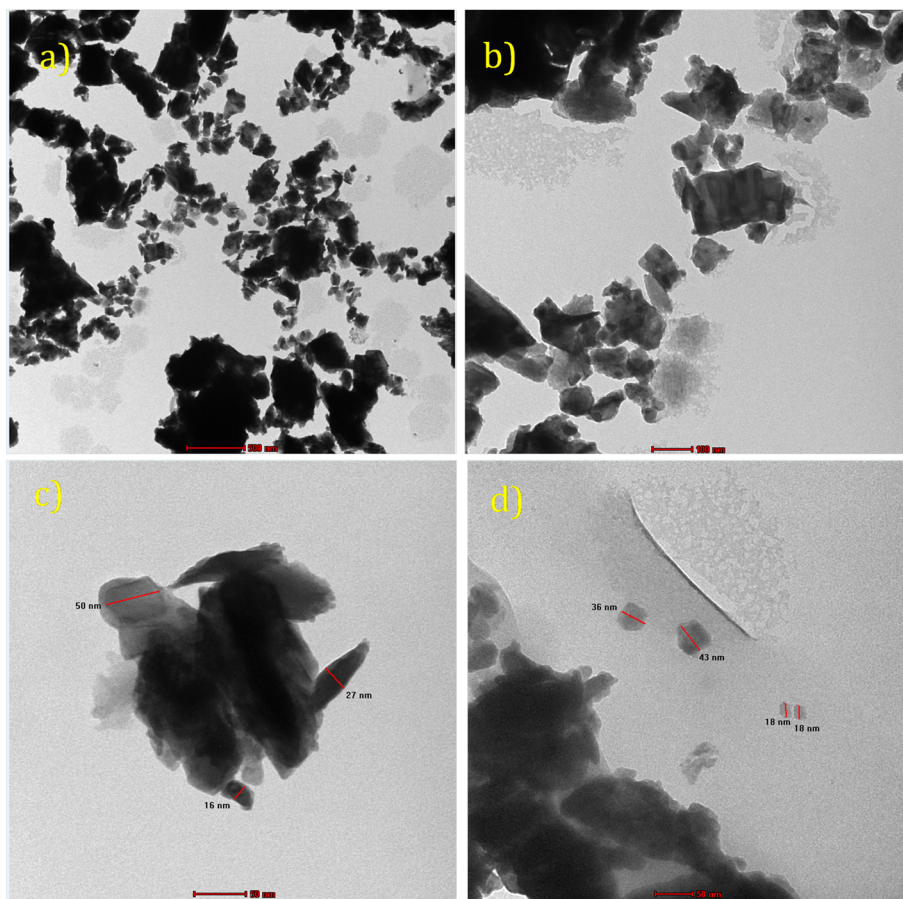


Fig. 4 TEM images of the prepared  $\text{Pr}_6\text{O}_{11}$  at different magnifications.

crystallite size of the praseodymium oxide nanoparticles ( $\text{Pr}_6\text{O}_{11}$  NPs) calculated by Scherrer's equation was 12.84 nm.

**4.1.2. FTIR analysis.** The FTIR spectra of the synthesized  $\text{Pr}_6\text{O}_{11}$  NPs were recorded to identify the functional groups. As shown in Fig. 1b, there was a peak around  $3600\text{ cm}^{-1}$ , corresponding to  $-\text{OH}$  stretching and bending vibrations from surface hydroxyl groups absorbed water molecules, while the peak around  $500\text{--}700\text{ cm}^{-1}$  could be attributed to  $\text{Pr}-\text{O}$  stretching vibrations, indicating the presence of  $\text{Pr}_6\text{O}_{11}$ . The peak around  $654\text{ cm}^{-1}$  was due to  $\text{Pr}-\text{O}-\text{Pr}$  bridging vibrations while the peak around  $508\text{ cm}^{-1}$  was related to  $\text{Pr}-\text{O}$  stretching modes.

**4.1.3. TGA and DTA analyses.** The thermo-gravimetric analysis (TGA) curve of  $\text{Pr}_6\text{O}_{11}$  NPs showed two distinct weight

loss steps (Fig. 1c). The first weight loss of approximately 7.2% in the temperature range  $50\text{--}354\text{ }^\circ\text{C}$  was attributed to the loss of physically adsorbed moisture from the surface of the nanoparticles. This was further supported by the corresponding endothermic peak observed in the DTA curve at a temperature of around  $250\text{ }^\circ\text{C}$ . The second weight loss, in the temperature range  $400\text{--}750\text{ }^\circ\text{C}$ , accounted for an additional 3% weight loss, which may indicate thermal decomposition or phase transformation within the oxide structure. The exothermic peak observed in the DTA curve during this temperature range suggested a release of energy, likely associated with the phase stabilization in  $\text{Pr}_6\text{O}_{11}$ .

**4.1.4. SEM and EDX analyses.** Fig. 2 displays the FESEM images of the  $\text{Pr}_6\text{O}_{11}$  NPs at four different magnifications.

Table 1 Screening of catalysts, solvents, and reaction conditions

Sr. no	Catalyst	Solvent	Temp. ( $^\circ\text{C}$ )	Time	Yield (%)
1	—	Water	RT	24	—
2	—	NaPTS (20%)	RT	3	Trace
3	$\text{Pr}_6\text{O}_{11}$ NPs	Water/NaPTS (20%)	$60\text{ }^\circ\text{C}$	30 min	60
4	$\text{Pr}_6\text{O}_{11}$ NPs	Water/NaPTS (20%)	RT	20 min	85
5	$\text{Pr}_6\text{O}_{11}$ NPs	$\text{EtOH}:\text{H}_2\text{O}$ (1 : 1)	RT	1	90
6	$\text{Pr}_6\text{O}_{11}$ NPs	Ethanol	RT	1	92
7	$\text{Pr}_6\text{O}_{11}$ NPs	Water/NaPTS (20%)	Ultrasound	5 min	96

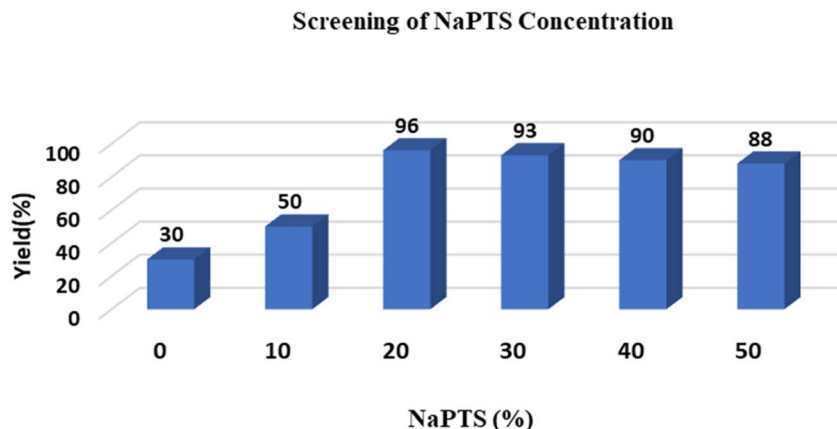


Fig. 5 Screening of the optimal concentration of NaPTS for the synthesis of chromene derivatives.

Table 2 Effect of  $\text{Pr}_6\text{O}_{11}$  NPs loading on the yield of the reaction model

Entry	Catalyst (mol %)	Catalyst (mol %)	Temp. (°C)	Time (min)	Yield 1 h (%)
1	$\text{Pr}_6\text{O}_{11}$ NPs	5 mol%	RT	40	65
2	$\text{Pr}_6\text{O}_{11}$ NPs	10 mol%	RT	5	96
3	$\text{Pr}_6\text{O}_{11}$ NPs	15 mol%	RT	20	82

Specifically, Fig. 2a depicts the NPs clusters at a magnification of  $500\times$ , illustrating their morphological structure. Fig. 2b–d also show clusters of NPs with morphological structures of irregular shapes at  $2000\times$ ,  $5000\times$ , and  $10\,000\times$  magnifications. The average  $\text{Pr}_6\text{O}_{11}$  NPs cluster size was in the 18–40 nm range. Furthermore, EDX confirmed the Pr and O in the catalysts.

The EDX spectrum is illustrated in Fig. 2e, showing the  $\text{Pr}_6\text{O}_{11}$  NPs consisted of the elements Pr and O, revealing that organic molecules were present in the  $\text{Pr}_6\text{O}_{11}$  NPs.

**4.1.5. BET analysis.** The BET study of the  $\text{Pr}_6\text{O}_{11}$  was performed by obtaining the nitrogen adsorption–desorption isotherms at 77 K, which demonstrated an H3 type hysteresis loop, indicating their slit-shaped or wedge-shaped pore formation, as observed in Fig. 3a. The pore-size distribution was narrow with no limiting adsorption at high values of  $P/P_0$ . Next,

a BJH study was carried out to evaluate the specific surface area and the average pore-size diameter. The  $\text{Pr}_6\text{O}_{11}$  nanoparticles had a specific surface area of  $9.677\text{ m}^2\text{ g}^{-1}$  and an average pore size of  $35.09\text{ nm}$  and pore volume of  $0.40\text{ cm}^3\text{ g}^{-1}$  (Fig. 3b). A high surface area and average pore size are more beneficial for enhancing the catalytic properties.

**4.1.6. TEM analysis.** The TEM image of  $\text{Pr}_6\text{O}_{11}$  NPs showed they were quasi-spherical nanoparticles with an average size 20 nm that were agglomerated together (Fig. 4a). Also some octahedral-shaped particles could be observed, which were due to salt impurities due to  $\text{PrCl}_3$  (Fig. 4d), albeit in trace quantities.

## 4.2. Study of chromene derivatives obtained using $\text{Pr}_6\text{O}_{11}$ NPs

The catalytic performance of  $\text{Pr}_6\text{O}_{11}$  NPs was evaluated for the synthesis of chromene derivatives using a model reaction with 4-methoxybenzaldehyde, malononitrile, and resorcinol. Initially, the reaction in an aqueous medium failed, while in ethanol, only a trace amount of the product was formed, indicating the need for a catalyst. When  $\text{Pr}_6\text{O}_{11}$  NPs were introduced, the reaction proceeded smoothly, leading to higher product yields. This study demonstrated that the  $\text{Pr}_6\text{O}_{11}$  NPs are effective catalysts, offering a promising approach for green chemistry applications.

Table 3 Comparison of  $\text{Pr}_6\text{O}_{11}$  with previously reported catalysts for the preparation of chromene derivatives

Sr. no	Catalyst	Solvent	Temp. (°C)	Time (min)	Yield (%)	References
1	L-Proline	EtOH : H <sub>2</sub> O (1 : 1)	60 °C	30	86–96	47
2	$\text{Na}_2\text{CO}_3$	Solvent-free	50 °C	40	92	48
3	Nano $\text{SiO}_2$	Water	70 °C	30	90	49
4	$\text{Fe}(\text{HSO}_4)_3$	$\text{CH}_3\text{CN}$	Reflux	4 h	83	32
5	ACDs	Water	RT	3 h	94	50
6	POPINO	Water	Reflux	15	92	51
7	Tungstic acid-SBA-15	Water	100 °C	12 h	86	52
8	Nano-cellulose- $\text{OTiCl}_3$	EtOH	Reflux	20	90	53
9	Polyoxometalate@dysprosium	EtOH : H <sub>2</sub> O	Reflux	15	90	54
10	$\text{Pr}_6\text{O}_{11}$	Water/NaPTS (20%)	Ultrasound	5	96	Present work



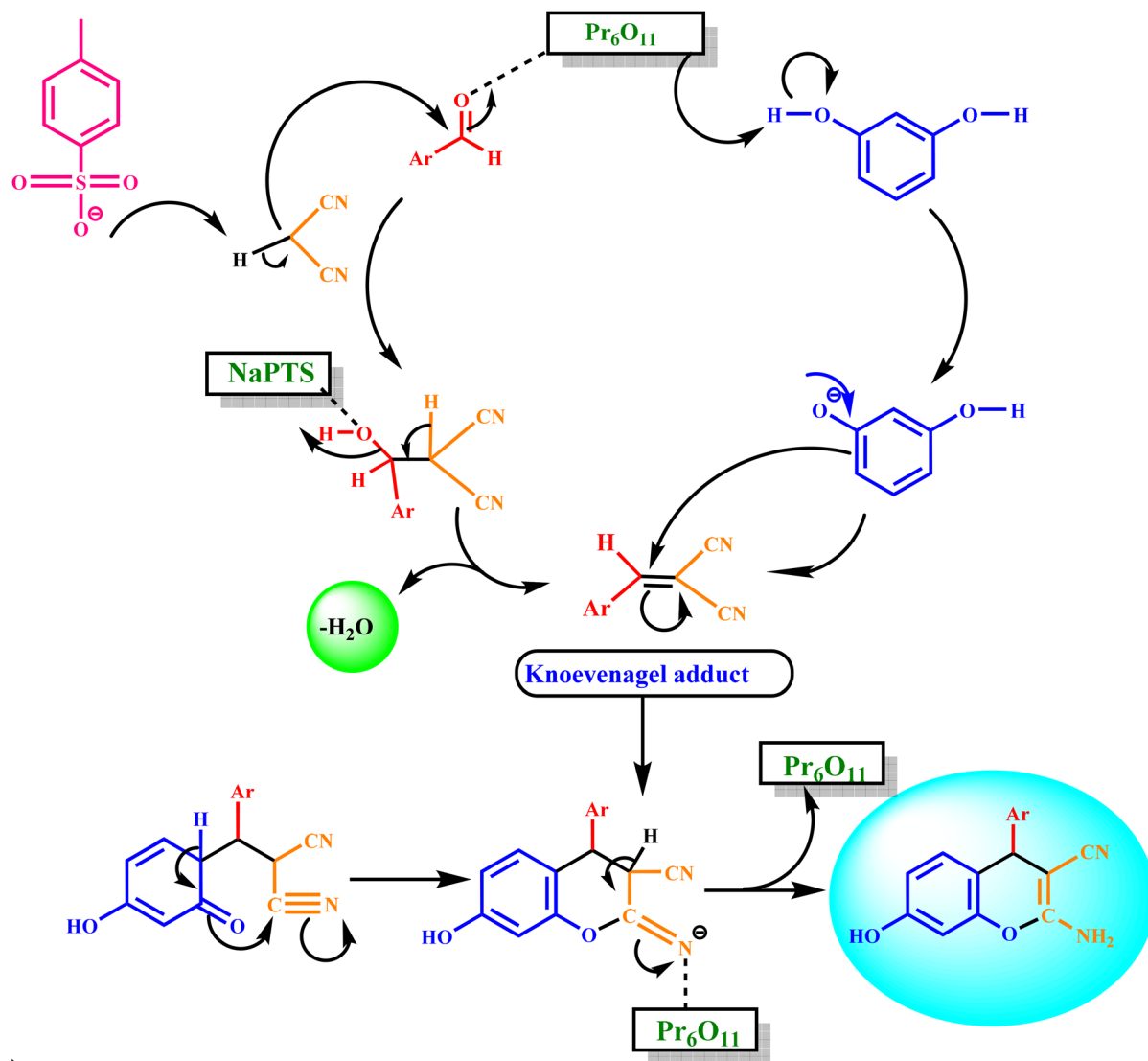
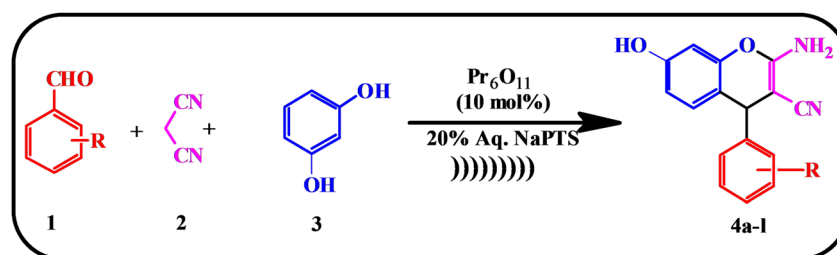


Fig. 6 Mechanism for the synthesis of chromene derivatives.

To improve the yield, ultrasonication was added to the model reaction, leading to better results than before. We also tested ethanol and ethanol/water with Pr<sub>6</sub>O<sub>11</sub> NPs, but these did not yield the desired results.

Table 1 and Fig. 5 shows that Pr<sub>6</sub>O<sub>11</sub> NPs in 20% NaPTS under ultrasound irradiation provided the optimal conditions for chromene synthesis. Specifically, 20% NaPTS played

a crucial role as a hydrotrope. Its primary function was to enhance the solubility of the hydrophobic organic substrates in water without forming micelles, like surfactants. This improved the reaction homogeneity and facilitated a better interaction between the reactants and the nanocatalyst in the aqueous phase. Additionally, NaPTS contributed to reducing the interfacial tension, which promoted more efficient mass transfer in



Scheme 1 Synthesis of chromene derivatives using Pr<sub>6</sub>O<sub>11</sub> nanoparticles.

Table 4 Synthesis of chromene derivatives

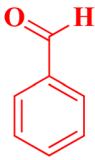
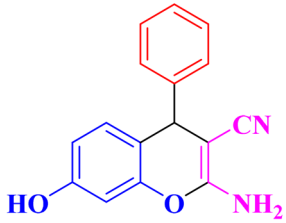
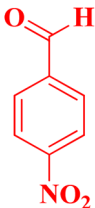
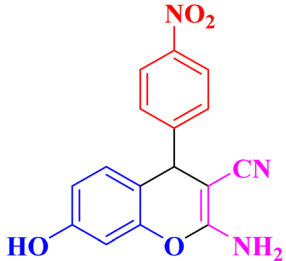
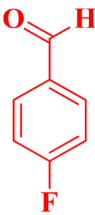
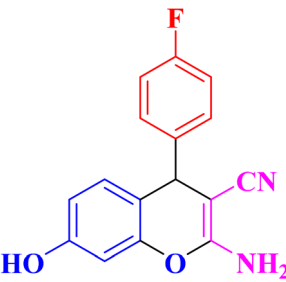
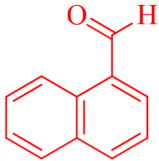
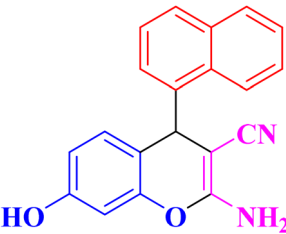
Entry	Aldehyde	Product	Time (min)	Yield (%)	Melting point (°C)	
					Obs.	Lit.
1		 <b>4a</b>	5	96	233	(234–236)
2		 <b>4b</b>	4	92	208	(209–210)
3		 <b>4c</b>	5	92	293	(293–294)
4		 <b>4d</b>	5	92	280	(278–280)



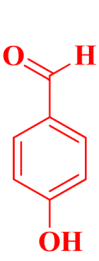
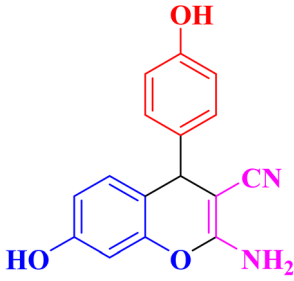
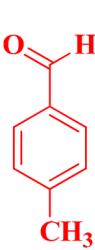
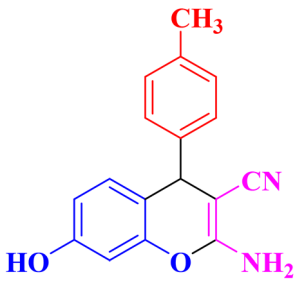
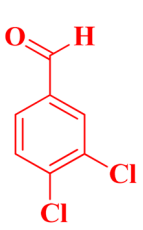
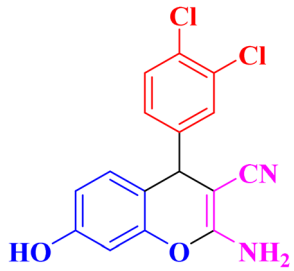
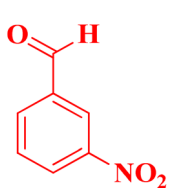
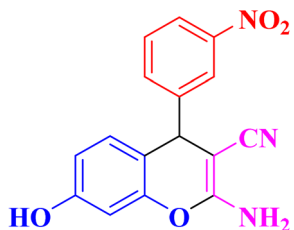


Table 4 (Contd.)

Entry	Aldehyde	Product	Time (min)	Yield (%)	Melting point (°C)	
					Obs.	Lit.
5			7	91	215	(213–215)
6			5	93	160	(160–162)
7			7	90	206	(207–209)
8			5	96	192	(192–194)



Table 4 (Contd.)

Entry	Aldehyde	Product	Time (min)	Yield (%)	Melting point (°C)	
					Obs.	Lit.
9		 <b>4i</b>	6	92	250	(248–250)
10		 <b>4j</b>	4	90	183	(182–183)
11		 <b>4k</b>	5	92	257	(256–258)
12		 <b>4l</b>	10	83	211	(211–214)

the heterogeneous aqueous system. It accelerated the reaction rates by creating a favorable microenvironment around the catalyst surface under ultrasound conditions. These parameters support green chemistry principles by avoiding the need to use

harmful organic solvents and enabling reactions to be carried out in water. Overall, NaPTS enhanced the sustainability, efficiency, and environmental compatibility of the synthetic protocol. The catalyst loading was further optimized using 20%



Table 5 Calculation of the green chemistry metrics

S. no.	Parameters	Formula	Characteristics	Ideal value	Calculated value for compound
1	Environmental ( <i>E</i> ) factor	$[\text{Total mass of the raw materials} - \text{the total mass of the product}] / \text{mass of the product}$	<i>E</i> -Factor shows the total amount of waste generated in a chemical reaction	0	$[(0.136 + 0.066 + 0.110) - 0.292] / 0.292 = 0.07$
2	Process mass intensity (PMI)	$\Sigma (\text{mass of materials}) / [\text{total mass of the isolated product}]$	PMI takes into account the reaction efficiency, stoichiometry, amount of solvent, and all the reagents used in the chemical reaction	1	$(0.136 + 0.066 + 0.110) / 0.292 = 1.06$
	Reaction mass efficiency (RME%)	$[\text{Product} / \Sigma (\text{mass of stoichiometric reactants})] \times 100$	RME accounts for the atom economy, chemical yield and stoichiometry	100%	$[0.292 / (0.136 + 0.066 + 0.110)] \times 100 = 93.58\%$

NaPTS, with the results shown in Table 2. Table 3 presents a comparative study between previously reported catalysts and the newly developed  $\text{Pr}_6\text{O}_{11}$  catalyst for the synthesis of chromene derivatives.

The best yield was achieved with 10 mol% of  $\text{Pr}_6\text{O}_{11}$  NPs. Hence, along with the other reaction parameters, it was considered as the optimized choice. The yield of the product was found to be decreased when the molar concentration of the catalyst was increased or decreased. This supports our hypothesis that the small size and porous structure of  $\text{Pr}_6\text{O}_{11}$  NPs offer more active sites (Fig. 6), facilitating faster reactions in the presence of the hydrotrope and ultrasound irradiation, leading to high yields at room temperature. Various chromene derivatives were synthesized using different aromatic aldehydes with the optimized catalyst loading in the hydrotropic aqueous medium (Scheme 1), and the results are summarized in Table 4.

### 4.3. Green chemistry matrix evaluation

**4.3.1. Process mass intensity.** In accordance with the principles of green chemistry, we evaluated several green metrics to assess the sustainability and efficiency of the developed protocol, which are shown in Table 5. A representative reaction involving 4-methoxybenzaldehyde, malononitrile, and resorcinol was used to calculate the reaction mass efficiency (RME), *E*-factor, and process mass intensity (PMI). The respective amounts of reactants used were 4-methoxybenzaldehyde (0.136 g, 1 mmol), malononitrile (0.066 g, 1 mmol), and resorcinol (0.110 g, 1 mmol). The reaction yielded 0.292 g (0.95 mmol) of the desired 2-amino-3-cyano-4*H*-chromene product.

These results indicate the high atom economy, excellent mass efficiency, and minimal waste generation of the developed protocol. The low *E*-factor and PMI value close to 1 highlight the environmental and economic sustainability of the process. The use of a non-toxic, recyclable catalyst in an aqueous hydrotropic

medium, along with high yields and short reaction times, further confirmed the green and efficient nature of the developed methodology.

**4.3.2. Atom economy.** The atom economy is a crucial metric in green chemistry. It assesses the efficiency of a chemical reaction by considering how much of the reactant mass is incorporated into the final product. It is expressed as a percentage and is calculated using the formula:

$$\text{Atom economy} = \frac{(\text{total molar mass of reactants} / \text{molar mass of desired product}) \times 100}{}$$

The atom economy values, as provided in Table 6, ranged from 87.95 to 90.86%, indicating that all these reactions were relatively efficient. A higher atom economy means fewer byproducts, leading to improved sustainability in chemical synthesis. In contrast, reactions with a lower atom economy may involve the loss of atoms as side products or leaving groups, making them less desirable from a green chemistry perspective.

Analyzing the data, entry 7 (90.86%) had the highest atom economy, suggesting that this reaction effectively incorporated most of the reactant atoms into the final product. This indicated a well-optimized reaction with minimal waste. On the other hand, entry 1 (87.95%) had the lowest atom economy, implying that some portion of the reactants was not utilized efficiently, possibly due to the formation of byproducts or side reactions. Other entries fell within this range, showing slight variations based on the nature of the reactants, reaction mechanisms, and functional groups involved. For example, reactions with halogenated compounds or protective groups might have slightly lower atom economies due to the elimination of non-contributing atoms during product formation.

Table 6 Atom economy of the synthesized chromene derivatives

Entry no.	1	2	3	4	5	6	7	8	9	10	11	12
Atom economy	87.95	89.60	88.67	89.76	90.06	89.26	90.86	89.11	88.59	88.52	90.31	89.60



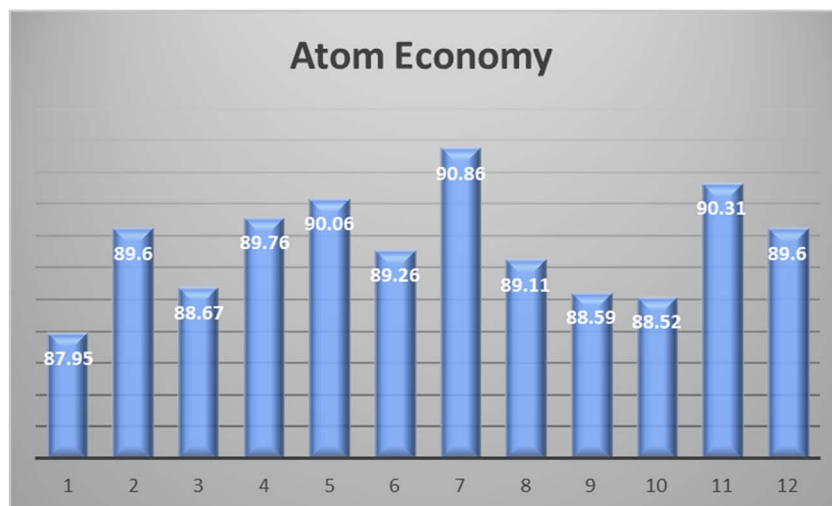


Fig. 7 The atom economy values for the synthesized chromene derivatives.

From a practical standpoint, reactions with a higher atom economy are highly desirable in industrial and pharmaceutical applications, as they reduce the need for extensive purification, lower the material costs, and decrease the environmental impact. Chemists can enhance the atom economy by selecting appropriate catalysts, designing atom-efficient synthetic routes, and utilizing solvent systems that promote complete reactant conversion. Fig. 7 indicates that all the reactions listed were relatively efficient, demonstrating good alignment with the principles of green chemistry. Further optimization could push these efficiencies even higher, contributing to more sustainable and economically viable chemical processes.

#### 4.4. Reproducibility and yield consistency

To validate the reproducibility and reliability of the developed protocol, the model reaction involving 4-methoxybenzaldehyde, malononitrile, and resorcinol was performed in triplicate under the optimized conditions. The product yields obtained in three independent experiments were 95%, 96%, and 94%,

respectively. The average yield was calculated as 95% with a standard deviation of  $\pm 1.0\%$ . These results confirm the excellent consistency and robustness of the catalytic system, supporting the claim of high reproducibility and the practical applicability of this green synthetic approach.

#### 4.5. Recyclability

Fig. 8 depicts a graph showing the yields obtained with increasing the number of uses of the  $\text{Pr}_6\text{O}_{11}$  catalyst. After each reaction, the catalyst was isolated by simple filtration, reactivated by cleaning with ethanol, and then dried in a hot air oven. The figure depicts the catalyst's stability and consistent performance over multiple cycles, whereby the product was separated by filtering the reaction mixture, the aqueous layer was recovered, and the organic layer was extracted using ethyl acetate. Compared to previous studies reported in the literature,<sup>18–30</sup> a key advantage of the present approach is the ability to reuse the  $\text{Pr}_6\text{O}_{11}$  NPs catalyst up to five times without significant loss in catalytic activity. The  $\text{Pr}_6\text{O}_{11}$  NPs after the

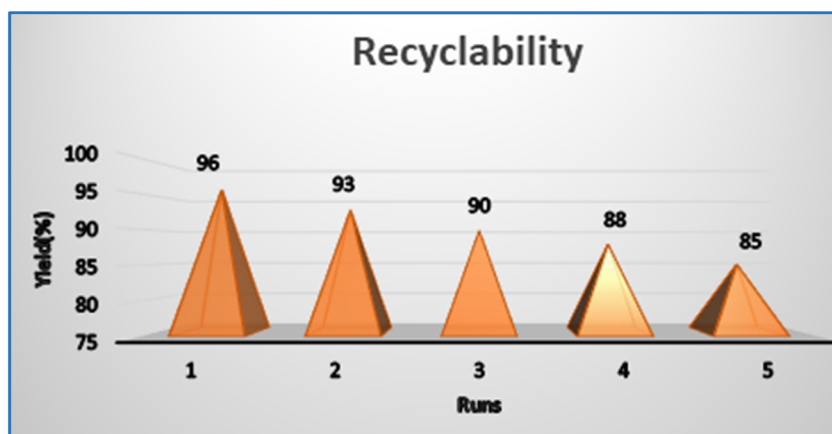


Fig. 8 Recyclability test of  $\text{Pr}_6\text{O}_{11}$  NPs.





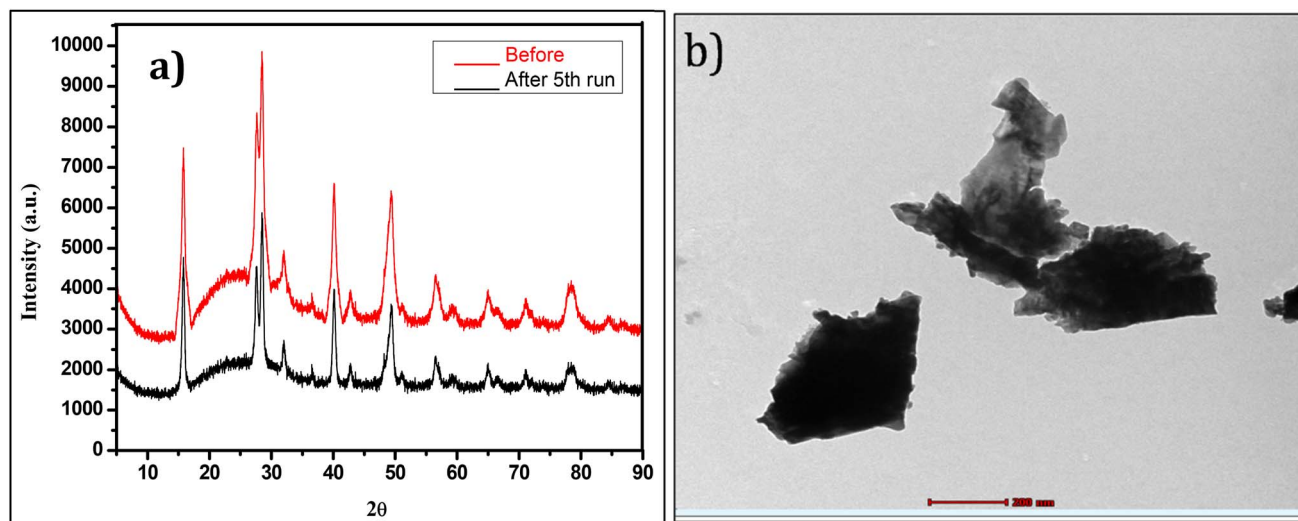


Fig. 9 (a) XRD spectrum of the  $\text{Pr}_6\text{O}_{11}$  NPs recycled after 5 cycles. (b) TEM image of  $\text{Pr}_6\text{O}_{11}$  NPs recycled after 5 cycles.

fifth reuse showed no significant changes, indicating that the catalyst retained its original properties.

#### 4.6. Before and after characterization of the catalyst

Fig. 9a shows the XRD patterns of the  $\text{Pr}_6\text{O}_{11}$  nanoparticles before and after the 5th catalytic cycle, indicating that their crystalline nature was well retained. A slight reduction in peak intensity suggested minor structural changes or surface passivation due to repeated use. Fig. 9b presents a TEM image of the  $\text{Pr}_6\text{O}_{11}$  nanoparticles after the 5th cycle, showing that the particles were aggregated but preserved their morphology, confirming the good structural stability and reusability of the catalyst.

## 5. Conclusion

The ultrasonic-assisted synthesis of 2-amino-4H-chromene derivatives was successfully achieved using hydrothermally synthesized  $\text{Pr}_6\text{O}_{11}$  nanoparticles as an efficient catalyst. The use of  $\text{Pr}_6\text{O}_{11}$  nanoparticles offers distinct advantages, enabling the facile and efficient synthesis of 2-amino-4H-chromene derivatives. Notably, the catalyst demonstrated excellent reusability, retaining up to 85% yield even after five consecutive cycles. Ultrasonic irradiation played a crucial role in the process by controlling the particle size and crystalline phases of the products, as well as facilitating rapid separation. Therefore, the integration of ultrasonication with  $\text{Pr}_6\text{O}_{11}$  nanoparticle catalysis represents a novel and effective approach for the synthesis and separation of 2-amino-4H-chromene derivatives.

## Data availability

Data will be available from the corresponding author upon reasonable request.

## Conflicts of interest

There are no conflicts to declare.

## References

- 1 *Multicomponent Reactions*, ed. J. Zhu, Wiley-VCH, Weinheim, 2005; S. Abdolmohammadi, *Curr. Catal.*, 2013, 2(2), 116–121; S. Abdolmohammadi and M. Afsharpour, *Z. Naturforsch., B: J. Chem. Sci.*, 2015, 70(3), 171–176; S. Abdolmohammadi, Z. Hossaini and R. Poor Heravi, *Mol. Diversity*, 2022, 26(4), 1983–1993.
- 2 J. Safari, Z. Zarnegar and M. Heydarian, Practical, ecofriendly, and highly efficient synthesis of 2-amino-4H-chromenes using nanocrystalline MgO as a reusable heterogeneous catalyst in aqueous media, *J. Taibah Univ. Sci.*, 2013, 7, 17–25, DOI: [10.1016/j.jtusci.2013.03.001](https://doi.org/10.1016/j.jtusci.2013.03.001).
- 3 S. Abdolmohammadi, Study of the Catalytic Activity of  $\text{Zr}(\text{HPO}_4)_2$  in the Synthesis of Hexahydroquinoline Derivatives under Solvent-free Conditions, *Z. Naturforsch. B Chem. Sci.*, 2013, 68, 195–200, DOI: [10.5560/zn.b.2013-2237](https://doi.org/10.5560/zn.b.2013-2237).
- 4 S. Abdolmohammadi,  $\alpha$ -ZrP: A Highly Efficient Catalyst for Solvent-free Synthesis of Pyrimido[5',4':5,6]pyrido[2,3-d]pyrimidin-4-one and 4-Arylacridinedione Derivatives, *Lett. Org. Chem.*, 2014, 11, 465–469, DOI: [10.2174/1570178611666140124002242](https://doi.org/10.2174/1570178611666140124002242).
- 5 S. Abdolmohammadi, Silica Supported  $\text{Zr}(\text{HSO}_4)_4$  Catalyzed Solvent-free Synthesis of [1]Benzopyrano[4,3-b][1]benzopyran-6-ones and Xanthenones, *Lett. Org. Chem.*, 2014, 11, 350–355, DOI: [10.2174/1570178610666131212231709](https://doi.org/10.2174/1570178610666131212231709).
- 6 S. Balalaie, S. Abdolmohammadi and B. Soleimanifard, An Efficient Synthesis of Novel Hexahydropyrido[2,3-d]pyrimidine Derivatives from (Arylmethylidene)pyruvic Acids (=(3 E)-4-Aryl-2-oxobut-3-enoic Acids) in Aqueous Media, *Helv. Chim. Acta*, 2009, 92, 932–936, DOI: [10.1002/hlca.200800318](https://doi.org/10.1002/hlca.200800318).
- 7 A. Kadam, N. Shirke, P. Gaikwad and S. Kamble, Embedded Nickel Complex on Naturally Biodegradable Gaur Gum: Catalytic Application for the Green Synthesis of 2-Amino-3-



- Cyano-7-Hydroxy-4 H -Chromenes, *Polycyclic Aromat. Compd.*, 2023, 1–13, DOI: [10.1080/10406638.2023.2273910](https://doi.org/10.1080/10406638.2023.2273910).
- 8 B. Baghernejad and M. Rostami Harzevili, Nano-cerium Oxide/Aluminum Oxide: An Efficient and Useful Catalyst for the Synthesis of Tetrahydro[a]xanthenes-11-one Derivatives, *Chem. Methodol.*, 2021, 5, 90–95, DOI: [10.22034/chemm.2021.119641](https://doi.org/10.22034/chemm.2021.119641).
  - 9 A. R. Moosavi-Zare, Z. Asgari, A. Zare, M. A. Zolfigol and M. Shekouhy, One pot synthesis of 1,2,4,5-tetrasubstituted-imidazoles catalyzed by trityl chloride in neutral media, *RSC Adv.*, 2014, 4, 60636–60639, DOI: [10.1039/C4RA10589C](https://doi.org/10.1039/C4RA10589C).
  - 10 S. Abdolmohammadi, H. Pirelahi, F. Balalaie and S. Balalaie, Efficient Synthesis Of Dihydrochromeno[4,3-B] Chromenone and Derivatives In Aqueous Media, *Heterocycl. Commun.*, 2010, 16, 13–20, DOI: [10.1515/HC.2010.16.1.13](https://doi.org/10.1515/HC.2010.16.1.13).
  - 11 *Green Chemistry: Designing Chemistry for the Environment*, ed. P. T. Anastas, and T. C. Williamson, American Chemical Society, Washington, DC, 1996, DOI: [10.1021/bk-1996-0626](https://doi.org/10.1021/bk-1996-0626).
  - 12 S. R. Attar, A. C. Sapkal, C. S. Bagade, V. B. Ghanwat and S. B. Kamble, Biogenic CuO NPs for synthesis of coumarin derivatives in hydrotropic aqueous medium, *Res. Chem. Intermed.*, 2023, 49, 2989–3004, DOI: [10.1007/s11164-023-05034-2](https://doi.org/10.1007/s11164-023-05034-2).
  - 13 S. Ebrahimiasl, F. Behmagham, S. Abdolmohammadi, R. N. Kojabad and E. Vessally, Recent advances in the application of nanometal catalysts for Glaser coupling, *Curr. Org. Chem.*, 2019, 23, 2489–2503.
  - 14 N. Thomas and S. M. Zachariah, Pharmacological activities of chromene derivatives: an overview, *Asian J. Pharm. Clin. Res.*, 2013, 6, 11–15.
  - 15 C. V. Subbareddy, S. Sundarrajan, A. Mohanapriya, R. Subashini and S. Shanmugam, Synthesis, antioxidant, antibacterial, solvatochromism and molecular docking studies of indolyl-4H-chromene-phenylprop-2-en-1-one derivatives, *J. Mol. Liq.*, 2018, 251, 296–307, DOI: [10.1016/j.molliq.2017.12.082](https://doi.org/10.1016/j.molliq.2017.12.082).
  - 16 M. M. Kandeel, A. M. Kamal, E. K. A. Abdelall and H. A. H. Elshemy, Synthesis of novel chromene derivatives of expected antitumor activity, *Eur. J. Med. Chem.*, 2013, 59, 183–193, DOI: [10.1016/j.ejmech.2012.11.011](https://doi.org/10.1016/j.ejmech.2012.11.011).
  - 17 V. Raj and J. Lee, 2H/4H-Chromenes—A Versatile Biologically Attractive Scaffold, *Front. Chem.*, 2020, 8, 623, DOI: [10.3389/fchem.2020.00623](https://doi.org/10.3389/fchem.2020.00623).
  - 18 A. S. Salman, N. A. Mahmoud, A. Abdel-Aziem, M. A. Mohamed and D. M. Elsis, Synthesis, Reactions and Antimicrobial Activity of Some New 3-Substituted Indole Derivatives, *Int. J. Org. Chem.*, 2015, 05, 81–99, DOI: [10.4236/ijoc.2015.52010](https://doi.org/10.4236/ijoc.2015.52010).
  - 19 B. F. Mirjalili, L. Zamani, K. Zomorodian, S. Khabnadideh, Z. Haghighijoo, Z. Malakotikhah, S. A. Ayatollahi Mousavi and S. Khojasteh, Synthesis, antifungal activity and docking study of 2-amino-4H-benzochromene-3-carbonitrile derivatives, *J. Mol. Struct.*, 2016, 1116, 102–108, DOI: [10.1016/j.molstruc.2016.03.002](https://doi.org/10.1016/j.molstruc.2016.03.002).
  - 20 M. T. Flavin, J. D. Rizzo, A. Khilevich, A. Kucherenko, A. K. Sheinkman, V. Vilaychack, L. Lin, W. Chen, E. M. Greenwood, T. Pengsuparp, J. M. Pezzuto, S. H. Hughes, T. M. Flavin, M. Cibulski, W. A. Boulanger, R. L. Shone and Z.-Q. Xu, Synthesis, Chromatographic Resolution, and Anti-Human Immunodeficiency Virus Activity of (±)-Calanolide A and Its Enantiomers, *J. Med. Chem.*, 1996, 39, 1303–1313, DOI: [10.1021/jm950797i](https://doi.org/10.1021/jm950797i).
  - 21 G. A. Reynolds and K. H. Drexhage, New coumarin dyes with rigidized structure for flashlamp-pumped dye lasers, *Opt. Commun.*, 1975, 13, 222–225, DOI: [10.1016/0030-4018\(75\)90085-1](https://doi.org/10.1016/0030-4018(75)90085-1).
  - 22 M. José Climent, A. Corma and S. Iborra, Homogeneous and heterogeneous catalysts for multicomponent reactions, *RSC Adv.*, 2012, 2, 16–58, DOI: [10.1039/C1RA00807B](https://doi.org/10.1039/C1RA00807B).
  - 23 M. Keshavarz, N. Iravani, M. H. Ahmadi Azghandi and S. Nazari, Ion-pair immobilization of l-proline anion onto cationic polymer support and a study of its catalytic activity as an efficient heterogeneous catalyst for the synthesis of 2-amino-4H-chromene derivatives, *Res. Chem. Intermed.*, 2016, 42, 4591–4604, DOI: [10.1007/s11164-015-2302-0](https://doi.org/10.1007/s11164-015-2302-0).
  - 24 F. Bigi, S. Carloni, L. Ferrari, R. Maggi, A. Mazzacani and G. Sartori, Clean synthesis in water. Part 2: Uncatalysed condensation reaction of Meldrum's acid and aldehydes, *Tetrahedron Lett.*, 2001, 42, 5203–5205, DOI: [10.1016/S0040-4039\(01\)00978-9](https://doi.org/10.1016/S0040-4039(01)00978-9).
  - 25 M. M. Heravi, K. Bakhtiari, V. Zadsirjan, F. F. Bamoharram and O. M. Heravi, Aqua mediated synthesis of substituted 2-amino-4H-chromenes catalyzed by green and reusable Preyssler heteropolyacid, *Bioorg. Med. Chem. Lett.*, 2007, 17, 4262–4265, DOI: [10.1016/j.bmcl.2007.05.023](https://doi.org/10.1016/j.bmcl.2007.05.023).
  - 26 M. Kidwai, S. Saxena, M. K. Rahman Khan and S. S. Thukral, Aqua mediated synthesis of substituted 2-amino-4H-chromenes and *in vitro* study as antibacterial agents, *Bioorg. Med. Chem. Lett.*, 2005, 15, 4295–4298, DOI: [10.1016/j.bmcl.2005.06.041](https://doi.org/10.1016/j.bmcl.2005.06.041).
  - 27 H. Kiyani and F. Ghorbani, Potassium phthalimide promoted green multicomponent tandem synthesis of 2-amino-4H-chromenes and 6-amino-4H-pyran-3-carboxylates, *J. Saudi Chem. Soc.*, 2014, 18, 689–701, DOI: [10.1016/j.jscs.2014.02.004](https://doi.org/10.1016/j.jscs.2014.02.004).
  - 28 R. Ballini, G. Bosica, M. L. Conforti, R. Maggi, A. Mazzacani, P. Righi and G. Sartori, Three-component process for the synthesis of 2-amino-2-chromenes in aqueous media, *Tetrahedron*, 2001, 57, 1395–1398, DOI: [10.1016/S0040-4020\(00\)01121-2](https://doi.org/10.1016/S0040-4020(00)01121-2).
  - 29 D. Kumar, V. B. Reddy, B. G. Mishra, R. K. Rana, M. N. Nadagouda and R. S. Varma, Nanosized magnesium oxide as catalyst for the rapid and green synthesis of substituted 2-amino-2-chromenes, *Tetrahedron*, 2007, 63, 3093–3097, DOI: [10.1016/j.tet.2007.02.019](https://doi.org/10.1016/j.tet.2007.02.019).
  - 30 R. Maggi, R. Ballini, G. Sartori and R. Sartorio, Basic alumina catalysed synthesis of substituted 2-amino-2-chromenes via three-component reaction, *Tetrahedron Lett.*, 2004, 45, 2297–2299, DOI: [10.1016/j.tetlet.2004.01.115](https://doi.org/10.1016/j.tetlet.2004.01.115); S. Abdolmohammadi and Z. Aghaei-Meybodi, *Comb. Chem. High Throughput Screening*, 2015, 18(9), 911–916; M. Kiani, S. Abdolmohammadi and S. Janitabar-Darzi, *J. Chem. Res.*, 2017, 41(6), 337–340; S. Abdolmohammadi, *Comb. Chem.*



- High Throughput Screening*, 2018, **21**(8), 594–601; S. Abdolmohammadi and M. Afsharpour, *Appl. Organomet. Chem.*, 2021, **35**(1), e6028.
- 31 M. P. Surpur, S. Kshirsagar and S. D. Samant, Exploitation of the catalytic efficacy of Mg/Al hydrotalcite for the rapid synthesis of 2-aminochromene derivatives *via* a multicomponent strategy in the presence of microwaves, *Tetrahedron Lett.*, 2009, **50**, 719–722, DOI: [10.1016/j.tetlet.2008.11.114](#).
  - 32 H. Eshghi, S. Damavandi and G. H. Zohuri, Efficient One-Pot Synthesis of 2-Amino-4 H -chromenes Catalyzed by Ferric Hydrogen Sulfate and Zr-Based Catalysts of FI, *Synth. React. Inorg., Met.-Org., Nano-Met. Chem.*, 2011, **41**, 1067–1073, DOI: [10.1080/15533174.2011.591347](#).
  - 33 S. Shinde, G. Rashinkar and R. Salunkhe, DABCO entrapped in agar-agar: A heterogeneous gelly catalyst for multi-component synthesis of 2-amino-4H-chromenes, *J. Mol. Liq.*, 2013, **178**, 122–126, DOI: [10.1016/j.molliq.2012.10.019](#).
  - 34 X. Yu, X. Hu and Z. Zhou, Green and Efficient One-Pot Synthesis of 2-Amino-3-phenylsulphonyl-4H-chromenes under Solvent-Free Conditions, *Iran. J. Chem. Chem. Eng.*, 2018, **37**, 31–38.
  - 35 S. K. Kundu and A. Bhaumik, Triazine-based porous organic polymer: a novel heterogeneous basic organocatalyst for facile one-pot synthesis of 2-amino-4H-chromenes, *RSC Adv.*, 2015, **5**, 32730–32739.
  - 36 M. Saikia and L. Saikia, Sulfonic acid-functionalized MIL-101(Cr) as a highly efficient heterogeneous catalyst for one-pot synthesis of 2-amino-4H-chromenes in aqueous medium, *RSC Adv.*, 2016, **6**, 15846–15853, DOI: [10.1039/C5RA28135K](#).
  - 37 A. Chanda and V. V. Fokin, Organic Synthesis “On Water,” *Chem. Rev.*, 2009, **109**, 725–748, DOI: [10.1021/cr800448q](#).
  - 38 A. M. Saleh and L. K. El-Khordagui, Hydrotropic agents: a new definition, *Int. J. Pharm.*, 1985, **24**, 231–238, DOI: [10.1016/0378-5173\(85\)90023-7](#).
  - 39 P. Gaikwad and S. Kamble, Microwave enhanced green and convenient synthesis of 2-amino-4H-chromenes in aqueous hydrotropic medium, *Curr. Res. Green Sustainable Chem.*, 2020, **3**, 100014, DOI: [10.1016/j.crgsc.2020.100014](#).
  - 40 N. Krishna Chandar and R. Jayavel, Structural, morphological and optical properties of solvothermally synthesized Pr(OH)<sub>3</sub> nanoparticles and calcined Pr<sub>6</sub>O<sub>11</sub> nanorods, *Mater. Res. Bull.*, 2014, **50**, 417–420, DOI: [10.1016/j.materresbull.2013.11.006](#).
  - 41 P. X. Huang, F. Wu, B. L. Zhu, G. R. Li, Y. L. Wang, X. P. Gao, H. Y. Zhu, T. Y. Yan, W. P. Huang, S. M. Zhang and D. Y. Song, Praseodymium Hydroxide and Oxide Nanorods and Au/Pr<sub>6</sub>O<sub>11</sub> Nanorod Catalysts for CO Oxidation, *J. Phys. Chem. B*, 2006, **110**, 1614–1620, DOI: [10.1021/jp055622r](#).
  - 42 B. M. Abu-Zied, Y. A. Mohamed and A. M. Asiri, Fabrication, characterization, and electrical conductivity properties of Pr<sub>6</sub>O<sub>11</sub> nanoparticles, *J. Rare Earths*, 2013, **31**, 701–708, DOI: [10.1016/S1002-0721\(12\)60345-7](#).
  - 43 Y. Kalpaklı, The effect of in-situ Pr<sub>6</sub>O<sub>11</sub> phase formation on photocatalytic Performance: Mono azo dye degradation, *Inorg. Chem. Commun.*, 2024, **159**, 111788, DOI: [10.1016/j.inoche.2023.111788](#).
  - 44 I. V. Machado, J. R. N. Dos Santos, M. A. P. Januario and A. G. Corrêa, Greener organic synthetic methods: Sonochemistry and heterogeneous catalysis promoted multicomponent reactions, *Ultrason. Sonochem.*, 2021, **78**, 105704, DOI: [10.1016/j.ultsonch.2021.105704](#).
  - 45 S. Kamble, A. Kumbhar, G. Rashinkar, M. Barge and R. Salunkhe, Ultrasound promoted efficient and green synthesis of β-amino carbonyl compounds in aqueous hydrotropic medium, *Ultrason. Sonochem.*, 2012, **19**, 812–815, DOI: [10.1016/j.ultsonch.2011.12.001](#).
  - 46 S. Majeed and S. A. Shivashankar, Pr<sub>6</sub>O<sub>11</sub> micro-spherical nano-assemblies: Microwave-assisted synthesis, characterization and optical properties, *Mater. Chem. Phys.*, 2013, **143**, 155–160, DOI: [10.1016/j.matchemphys.2013.08.042](#).
  - 47 Z. Moghadasi, One-pot synthesis of 2-amino-4H-chromenes using L-proline as a reusable catalyst, *J. Med. Chem. Sci.*, 2019, **2**(1), 35–37.
  - 48 S. Javanshir, M. Safari and M. G. Dekamin, A facile and green three-component synthesis of 2-amino-3-cyano-7-hydroxy-4H-chromenes on grinding, *Sci. Iran.*, 2014, 742–747.
  - 49 F. Mohamadpour, Nano-SiO<sub>2</sub> as a reusable nanocatalyst promoted green synthesis of 2-amino-4H-chromenes in an aqueous solution, *Biointerface Res. Appl. Chem.*, 2022, **13**, 410–421.
  - 50 Y. Ren, B. Yang and X. Liao, The amino side chains do matter: chemoselectivity in the one-pot three-component synthesis of 2-amino-4H-chromenes by supramolecular catalysis with amino-appended β-cyclodextrins (ACDs) in water, *Catal. Sci. Technol.*, 2016, **6**, 4283–4293, DOI: [10.1039/C5CY01888A](#).
  - 51 M. G. Dekamin, M. Eslami and A. Maleki, Potassium phthalimide-N-oxyl: a novel, efficient, and simple organocatalyst for the one-pot three-component synthesis of various 2-amino-4H-chromene derivatives in water, *Tetrahedron*, 2013, **69**, 1074–1085, DOI: [10.1016/j.tet.2012.11.068](#).
  - 52 S. K. Kundu, J. Mondal and A. Bhaumik, Tungstic acid functionalized mesoporous SBA-15: A novel heterogeneous catalyst for facile one-pot synthesis of 2-amino-4H-chromenes in aqueous medium, *Dalton Trans.*, 2013, **42**, 10515, DOI: [10.1039/c3dt50947h](#).
  - 53 B. Sadeghi, E. Arabian and E. Akbarzadeh, Nano-cellulose-OTiCl<sub>3</sub> as a green and efficient catalyst for one-pot synthesis of 2-amino-7-hydroxy-4-aryl-4 H -chromene-3-carbonitrile, *Inorg. Nano-Met. Chem.*, 2020, **50**, 1207–1212, DOI: [10.1080/24701556.2020.1739076](#).
  - 54 S. Hosseinzadeh-Baghan, M. Mirzaei, H. Eshtiagh-Hosseini, V. Zadsirjan, M. M. Heravi and J. T. Mague, An inorganic-organic hybrid material based on a Keggin-type polyoxometalate@Dysprosium as an effective and green catalyst in the synthesis of 2-amino-4 H -chromenes *via* multicomponent reactions, *Appl. Organomet. Chem.*, 2020, **34**, e5793, DOI: [10.1002/aoc.5793](#).

